# Process study on the formation of nanocrystalline α-alumina with novel morphology at 1000 °C

Xiaoxue Zhang,*[a] Yanling Ge,[b] Simo-Pekka Hannula,[b] Erkki Levänen[a] and Tapio Mäntylä[a]

*Received 4th November 2008, Accepted 5th January 2009*
*First published as an Advance Article on the web 11th February 2009*
**DOI: 10.1039/b819592g**



We have reported in a short communication that nanocrystalline α-alumina with novel morphology was synthesized at a relatively low temperature of 1000 °C without any seed material. The α-alumina nanocrystallites at a size of 5 nm were observed for the first time, and more interestingly the nanocrystallites organized themselves into nanorods having widths of about 15 nm and lengths of about 50–250 nm. In this follow up full paper, detailed processing parameters of such nanocrystalline α-alumina are reported and more characterizations are carried out in order to study the mechanism of the synthesis. The formation scheme of the novel morphology of such nanocrystalline α-alumina is illustrated and the phase transformation from transition aluminas to α-alumina is discussed.

## 1. Introduction

It is well known that α-alumina has a high melting point, high thermal stability, high chemical inactivity and high hardness. As one of the most important ceramic materials, α-alumina has been widely used in many applications in microelectronics, refractories, optics and lasers, based on its mechanical, electrical and optical properties.[1] The synthesis of nanocrystalline ceramics is widely studied due to the belief that the mechanical properties of ceramics can be improved by the formation of a nanocrystalline structure.[2] Therefore, nanocrystalline α-alumina can be predicted to have improved properties compared to its micro and macro counterparts. To prepare α-alumina, nanocrystalline boehmite (AlOOH) or pseudo boehmite is a usual starting material. By calcination, it passes through the following series of phase transformations:[3]

$$\text{Boehmite} \rightarrow \gamma\text{-} \rightarrow \delta\text{-} \rightarrow \theta\text{-} \rightarrow \alpha\text{-alumina}$$

Methods to synthesize nanocrystalline boehmite include sol–gel processing,[4] hydrothermal method,[5] solvothermal method,[6] hydrolysis of aluminium metal,[7] steam-assisted solid wet-gel process[8] *etc*. By calcining such boehmite, nanocrystalline γ-alumina with rod-shaped morphology is commonly reported. However, only a limited number of papers have been published concerning synthesis of nanocrystalline α-alumina.[9,10] On the other hand, many speculations have been reported in the literature claiming the difficulties to obtain nanocrystalline α-alumina.[11–13] Furthermore, most of the reported small-sized α-alumina is spherical in shape and there are no reports of nanocrystallites of α-alumina less than 20 nm.

Meanwhile, the formation temperature of α-alumina has also been an intensive research topic. The phase transformation from θ-alumina to α-alumina involves a change in the oxygen sublattice from cubic to hexagonal close packing and generally happens above ~1200 °C.[14] Many efforts have been done to lower the formation temperature of α-alumina. Messing *et al.* firstly reported to add fine α-alumina[15] in 1984 and later α-$Fe_2O_3$[16] *via* a sol–gel process to provide heterogeneous nucleation sites for α-alumina to lower the phase transformation temperature to 1100 °C. After that, seeding material such as $AlF_3$[2] and alumina sol[17] has also been reported to lower the α-alumina formation temperature to around 1000 °C.

The sol–gel method is one of the most popular solution-based methods to synthesize α-alumina, which involves the formation of amorphous gel from a precursor solution. The sol–gel method is a well-known chemical synthesis route with high purity, high chemical homogeneity, lower calcination temperatures and good control of particle size.[18] The conventional process consists of three main steps: hydrolysis of the starting organometallics in particular alkoxides, gel formation and finally the calcination of the dried gel. The sol–gel method is a versatile method not only to synthesize nanoparticles[19] but also nanostructured functional thin films on various substrates.[20–22]

By modifying the conventional sol–gel process, we have reported the synthesis of nanocrystalline α-alumina with novel morphology in a previous short communication at a relatively low temperature of 1000 °C without any seeding material by calcining the novelly produced boehmite.[23] The α-alumina nanocrystallites at a size of 5 nm were observed for the first time, and more interestingly the 5 nm-nanocrystallites organize themselves into nanorods with widths of about 15 nm and lengths of about 50–250 nm. Nanocrystalline boehmite has been commonly synthesized, however, nanocrystalline α-alumina with such novel morphology obtained by calcining boehmite at 1000 °C without any seeding material has rarely been reported. In this follow up full paper, we have reported systematically the processing parameters of such nanocrystalline α-alumina. The phase transformation to α-alumina cannot be completed at 900 °C even with a very long dwell time of 160 h. On the other hand, above 1000 °C, only a shorter dwell time is required to obtain a pure phase of α-alumina at higher calcination temperatures *e.g.* calcination for

[a]*Department of Materials Science, Tampere University of Technology, P.O. Box 589, FI-33101 Tampere, Finland. E-mail: xiaoxue.zhang@tut.fi; Fax: +358 3 3115 2330; Tel: +358 40 849 0197*
[b]*Department of Materials Science and Engineering, Helsinki University of Technology, P.O. Box 6200, FI-02015 TKK, Finland*

1 h at 1100 °C results in a pure phase of α-alumina. We have also investigated a number of samples to determine the morphology and revealed that the starting boehmite powder and the transition alumina prepared by calcining the starting boehmite powder have similar morphology with the obtained nanocrystalline α-alumina at 1000 °C. The morphology of the starting boehmite powder plays an important role in the morphology of the obtained nanocrystalline α-alumina at 1000 °C, which is illustrated by a formation scheme of the novel morphology. Finally, we have discussed the phase transformation mechanism from θ-alumina to α-alumina and found that the diffusional nucleation model seems to be consistent with our results.

## 2. Experimental

The raw materials are aluminium tri-sec-butoxide (denoted as $Al(O\text{-}sec\text{-}Bu)_3$, $C_{12}H_{27}AlO_3$ > 97%, VWR), isopropyl alcohol (denoted as i-PrOH, $C_3H_7OH$ > 99%, VWR) and ethyl acetoacetate (denoted as EAcAc, $C_6H_{10}O_3$ > 98%, VWR). The procedures to prepare the sol–gel precursor were reported in a previous study.[23] By drying the precursor at 120 °C, a fine powder was obtained. The powder was then reacted with boiling water for 10 min to form boehmite (AlOOH). The boehmite-containing suspension was then dried at 120 °C to obtain fine boehmite powder, which was the starting material for the following calcinations. The calcinations were carried out in a tube furnace at 900 °C from 90 h to 160 h, at 1000 °C from 1 h to 40 h, as well as at 1100 °C from 0.5 h to 1 h in air atmosphere with a heating rate of 13 °C/min and cooling in furnace.

Crystalline phase was determined by a powder X-ray diffraction (XRD) pattern (Kristalloflex D-500, Simens) using Cu Kα radiation. The XRD pattern was measured from $2\theta$ range from 20° to 80° with a step size of 0.01° and a count time of 1 s per step. The average crystallite size $d_{XRD}$ was evaluated from an XRD pattern by using Scherrer equation, $d_{XRD} = K\lambda/(\text{FWHM})\cos\theta$, where $K = 0.9$, $\lambda = 1.5406$ Å, FWHM is the full width at the half maximum and $\theta$ is the glancing angle. The strongest diffraction peak of different aluminas was used to evaluate $d_{XRD}$. $N_2$ adsorption/desorption isotherms were obtained by using a gas sorption experiment (Coulter Omnisorp 100 CX, Beckman Coulter Inc.) at the temperature of liquid nitrogen. The samples were degassed at 200 °C prior to the measurement. The data analysis was carried out with Coulter SA-reports™ software. The specific surface areas were calculated by the Brunauer-Emmett-Teller (BET) equation using the data in a $P/P_0$ range of 0.05–0.4. The pore size distribution in meso range (3–100 nm) was obtained by a Barett-Joyner-Halenda (BJH) model from the desorption branches of the isotherms. The particle size $d_{BET}$ was evaluated by using equation $d_{BET} = 6/(\rho S_{ssa})$ where $\rho$ is the density of the solid and $S_{ssa}$ is the specific surface area, assuming the particles to be spherical or cubic. $N_2$ is generally considered to be the most suitable adsorptive for surface area determination, while for the solids of small specific surface areas (<5 $m^2/g$), Kr or Xe are said to be preferably used since they offer the possibility of higher precision in the measurement, however they do not necessarily give higher accuracy in the value of the surface area than that obtained with $N_2$.[24] Morphology and phase structure of the samples was studied by a high resolution transmission electron microscope (HRTEM, Tecnai F20 S-Twin). The fast Fourier transform (FFT) analysis of the HRTEM images was carried out by image analysis software, Gatan DigitalMicrograph Suite.

## 3. Results and discussion

### 3.1 Phase analysis

XRD patterns of the aluminas obtained by calcining the boehmite starting powder at 900 °C, 1000 °C and 1100 °C are

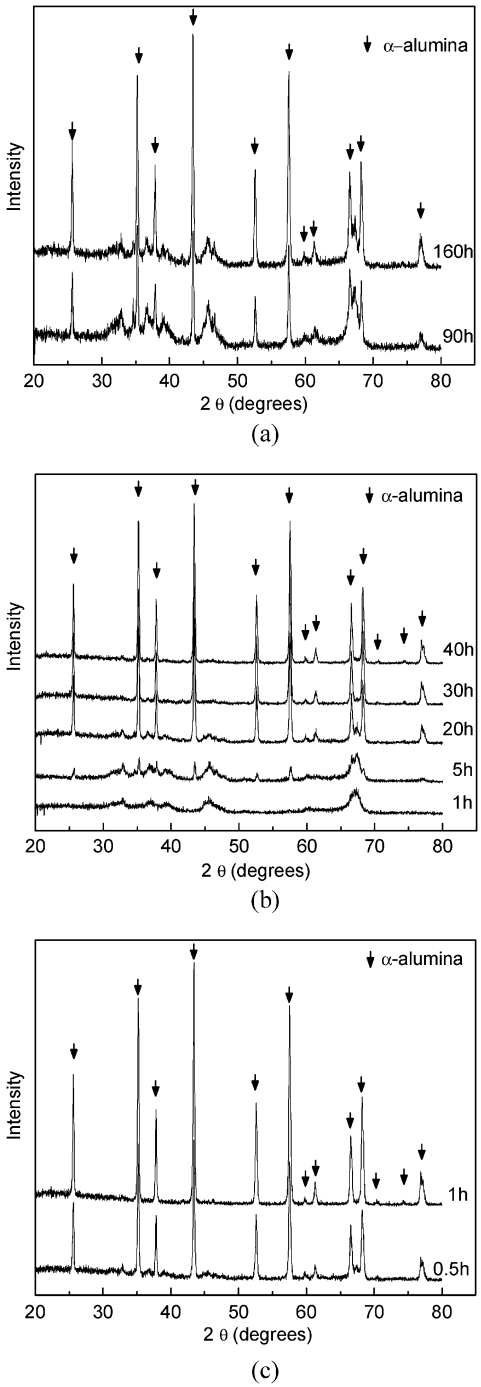


**Fig. 1** XRD patterns of the aluminas obtained by calcining the boehmite starting powder at 900 °C (a), 1000 °C (b) and 1100 °C (c) for different hours.

 

**Table 1** The crystalline phase, evaluated $d_{XRD}$, BET surface area and evaluated $d_{BET}$ of the boehmite starting powder and the obtained aluminas by calcining the boehmite powder at different temperatures for varying hours

| | | | 600 °C | 900 °C | | | 1000 °C | | | | | 1100 °C | | | |
|---|---|---|---|---|---|---|---|---|---|---|---|---|---|---|---|
| | *AlOOH*[13] | | 6 h[13] | 90 h | | 160 h | 1 h | 5 h | 20 h | | 30 h | 40 h | 0.5 h | | 1 h |
| Phase | *AlOOH* | γ | | δ,θ,*α* | | δ,θ,*α* | δ,θ | δ,θ,*α* | δ,θ,*α* | | θ,*α* | *α* | δ,θ,*α* | | *α* |
| $d_{XRD}$ (nm) | *3.9* | 4.0 | | 6.2(δ,θ)33(*α*) | | 7.5(δ,θ)33(*α*) | 5.9 (δ,θ) | 6.6(δ,θ)28(*α*) | 12(δ,θ)32(*α*) | | 13(θ)13(*α*) | 50 | 13(δ,θ)32(*α*) | | 36 |
| BET ($m^2/g$) | *303* | 320 | | 61 | | 36 | 79 | 66 | 26 | | 10 | 8.2 | 14 | | 8.1 |
| $d_{BET}$ (nm) | *6.6* | 5.9 | | [31(δ)] [28(θ)] [25(*α*)] | | [52(δ)] [47(θ)] [42(*α*)] | [24(δ)] [21(θ)] | [28(δ)] [25(θ)] [23(*α*)] | [72(δ)] [65(θ)] [58(*α*)] | | [169(θ)] [151(*α*)] | 184 | [134(δ)] [120(θ)] [108(*α*)] | | 186 |

shown in Fig. 1, where the arrows signify the peaks of α-alumina according to the JCPDS data (card No. 10–173). The alumina phases obtained at different temperatures for varying dwell hours are summarized in Table 1, together with the evaluated $d_{XRD}$. The data of the boehmite starting powder and the γ-alumina[19] obtained by calcining the boehmite starting powder at 600 °C for 6 h is also included in Table 1. At 900 °C for 90 h, α-alumina coexisted with δ- and θ-alumina. The intensities of the α-alumina peaks were increased when the boehmite was calcined at 900 °C for 160 h, however, the transformation to α-alumina was not complete and some amount of δ- and θ-alumina still existed in the sample. In other words, pure α-alumina was not obtained by the calcination at 900 °C even for the very long dwell time of 160 h. When the temperature was increased to 1000 °C, no peaks of α-alumina were observed with the dwell time of 1 h, and the sample was a mixture of δ- and θ-alumina, perhaps also γ-alumina.[19] For 5 h, α-alumina started to form with the coexistence of δ- and θ-alumina. For 20 h and 30 h, more and more α-alumina was formed, and for 40 h, the transformation to α-alumina was finally completed. When the temperature was further increased to 1100 °C, δ- and θ-alumina coexisted with α-alumina for 0.5 h while pure α-alumina was formed for 1 h.

To conclude from these XRD patterns, formation of pure α-alumina requires a calcination temperature of 1000 °C, at least. Less than 1000 °C, the transformation to α-alumina cannot be completed even with a very long dwell time. With a calcination temperature higher than 1000 °C, pure α-alumina can be achieved with a much shorter dwell time, for example 1 h at 1100 °C.

### 3.2 Porosity analysis

The $N_2$ adsorption/desorption isotherms and the corresponding pore size distribution of the aluminas prepared by calcining the boehmite starting powder at 900 °C, 1000 °C and 1100 °C are shown in Figs. 2–4. The specific surface area and the evaluated particle size $d_{BET}$ of the samples are also listed in Table 1, together with that of the boehmite starting powder and the γ-alumina obtained by calcining the boehmite powder at 600 °C for 6 h. When the sample is a mixture of different alumina phases, $d_{BET}$ is evaluated by using the density of different alumina phases which is indicated inside the parenthesis in Table 1. The shape of the isotherms, hysteresis loops and pore size distribution curves can be related with the phase transformation of transition alumina to α-alumina. When the boehmite was calcined at 900 °C for 90 h and 160 h, α-alumina coexisted with δ- and θ-alumina, and the isotherms and pore size distribution curves are shown in Fig. 2. Both isotherms are type IV isotherms with H2 hysteresis loops. The type IV isotherm is related to mesoporous structure; however, the samples also have some micropores indicated by the adsorption at very low relative pressure. The H2 hysteresis loop is believed to occur in the systems where the pores have narrow necks and wide bodies (*i.e.* "ink-bottle") or when the porous material has an interconnected pore network.[25] The bimodal pore size distribution has a narrow pore distribution around 6 nm and a broad pore distribution from 20 to 100 nm. The pore size distribution at around 6 nm is possibly due to the δ- and θ-alumina, which agrees well with their crystallites in sizes of 6.2 nm and 7.5 nm for 90 h and 160 h, see Table 1. On the other hand, the wide pore size distribution from 20–100 nm possibly

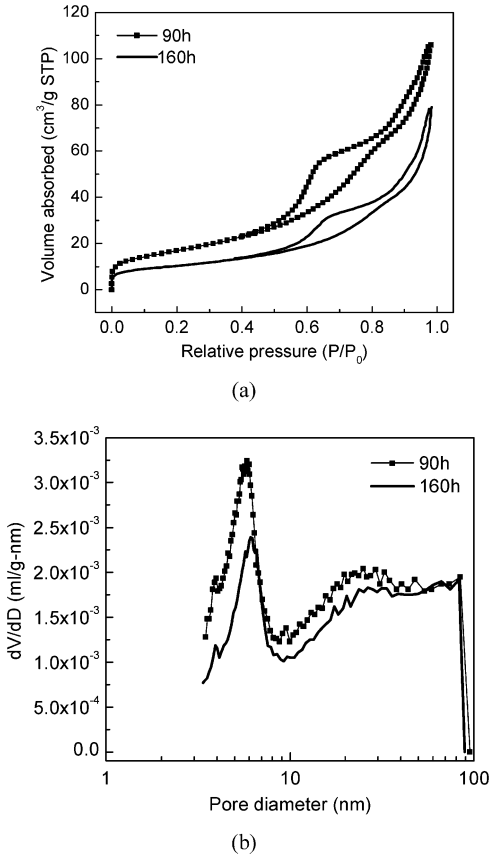


**Fig. 2** $N_2$ adsorption/desorption isotherms (a) and the corresponding pore diameter distribution (b) of the aluminas prepared by calcining the boehmite starting powder at 900 °C for 90 h and 160 h.

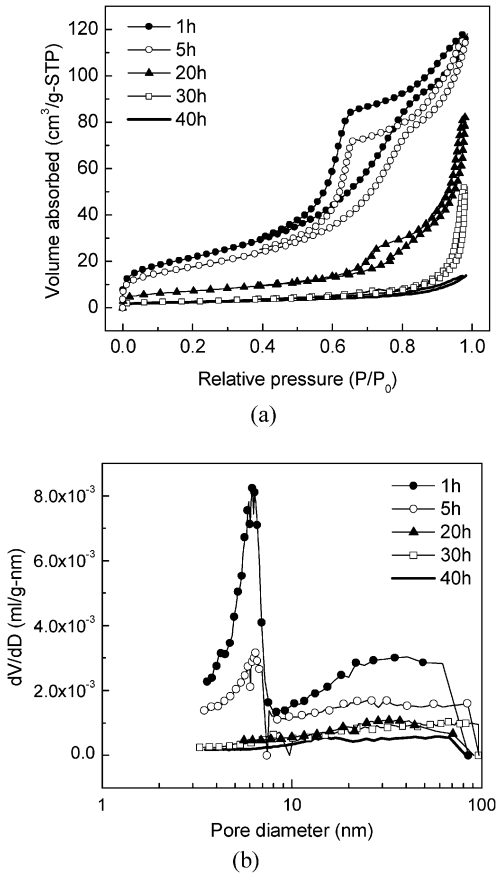


**Fig. 3** $N_2$ adsorption/desorption isotherms (a) and the corresponding pore diameter distribution (b) of the aluminas obtained by calcining the boehmite starting powder at 1000 °C from 1 h to 40 h.

results from the intercrystallite spaces of the δ-, θ- and α-alumina which has crystallites in the size of 33 nm. With the increase of the dwell time from 90 h to 160 h, the specific surface area is decreased from 61 to 36 $cm^2/g$. This is due to the increase in the amount of α-alumina and the decease in the amount of δ- and θ-alumina. Since the crystallite size of the aluminas remains quite the same for 90 h and 160 h, the pore size distribution curves are very similar.

The isotherms and pore size distribution curves of the aluminas prepared by calcining the boehmite starting powder at 1000 °C from 1 h to 40 h are shown in Fig. 3. All the isotherms are type IV isotherms, which are related to the mesopores in the samples. The hysteresis loops are type H2 for the samples of 1 h and 5 h, which also have micropores indicated from the adsorption at very low relative pressure. This can also be seen from their pore size distribution curves, in which the pore size distributions of both are bimodal with narrow distributions centred on 6 nm and wide distributions from 10 to 100 nm. The pore size distribution around 6 nm is due to the δ- and θ-alumina, which agrees well with their crystallites in sizes of 5.9 nm and 6.6 nm for 1 h and 5 h, see Table 1. The wide pore size distribution from 10 to 100 nm of the sample for 1 h is mainly from the interspaces between the transition alumina nanorods (see Fig. 6) since no α-alumina was formed. For 5 h, α-alumina started to form, which led to a decrease in the specific surface area and a broadening of the pore size distribution curve. When the time increased to 20 h and 30 h, the amount of α-alumina was increased and the δ- and θ-alumina grew to larger sizes of 12 and 13 nm, resulting in a further decrease in the specific surface area and the disappearance of the pore size distribution around 6 nm. However, the isotherms still have H2 hysteresis loops, although the hysteresis loop of the sample for 30 h looks very similar to the H3 hysteresis loop. When the dwell time was increased to 40 h, the phase transformation to α-alumina was finally completed. The isotherm has a H4 hysteresis loop with a wide distribution of mesopores. The H4 hysteresis loop is related with slit-shaped pores.[26]

When the boehmite starting powder was calcined at 1100 °C for 0.5 h, α-alumina coexisted with δ- and θ-alumina and the isotherm is type IV with a H2 hysteresis loop, see Fig. 4. The pore distribution is bimodal with a narrow distribution around 8 nm and a broad distribution from 10 nm to 100 nm. When the time increased to 1 h, pure α-alumina was obtained and the isotherm is type IV but with a H3 hysteresis loop. The H3 hysteresis loop is usually found in solids composed of aggregates or agglomerates of particles forming slit-shaped pores.[27] The pore size distribution is monomodal from 10 nm to 100 nm.

In all the cases, with the increases of calcination temperatures and dwell time, the specific surface area decreases and pore diameter increases due to the grain growth of transition alumina, phase transformation to α-alumina and its grain growth. When

 

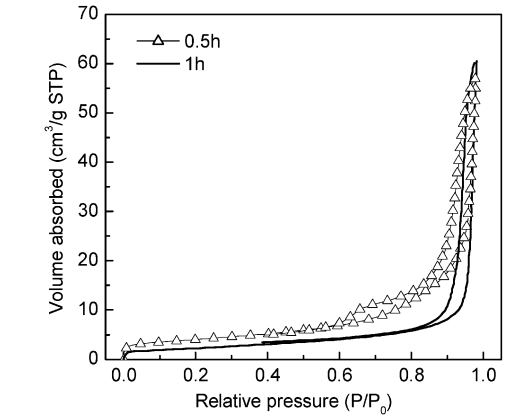


(a)

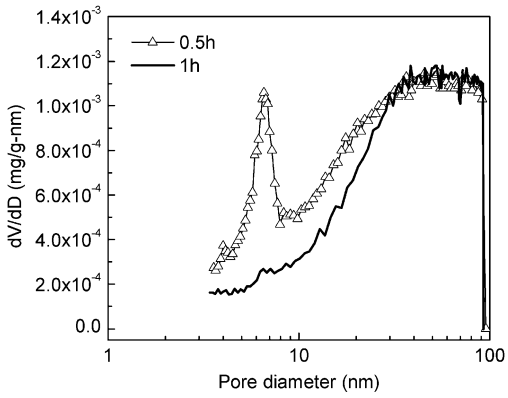


(b)

**Fig. 4** $N_2$ adsorption/desorption isotherms (a) and the corresponding pore diameter distribution (b) of the aluminas prepared by calcining the boehmite starting powder at 1100 °C for 0.5 h and 1 h.

transition aluminas and α-alumina coexisted, the isotherm is type IV with a H2 hysteresis loop, presenting a bimodal pore distribution. When pure α-alumina was obtained at 1000 °C and 1100 °C, the isotherms remain to be type IV, but with H4 and H3 hysteresis loops which both are related with slit-shaped pores. The pore structure change is due to the phase change from transition alumina to α-alumina. The evaluated $d_{BET}$ was larger than the $d_{XRD}$ resulting from the agglomeration and aggregation of the crystallites.

### 3.3 Morphology analysis

We have reported the novel morphology earlier of the nanocrystalline α-alumina obtained at 1000 °C for 40 h, in which the 5 nm crystallites form themselves into nanorods.[23] To understand the formation scheme of such novel morphology, more samples were studied by HRTEM. The TEM images of the γ-alumina obtained by calcining the boehmite powder at 600 °C for 6 h are shown in Fig. 5, where the image (a) was taken at low magnification and (b) at high magnification. The γ-alumina has the morphology of nanorods with the length of about 300 nm and the width of 10 nm. However, in the image (b), crystallites of 4 nm in size are observed, and the crystallites also form

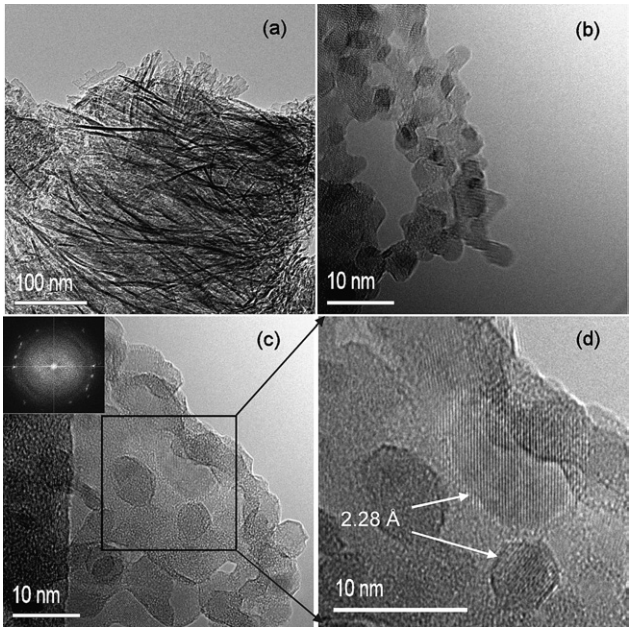


**Fig. 5** TEM studies of the alumina obtained by calcining the boehmite starting powder at 600 °C for 6 h. The FFT pattern of (c) is inserted and indexed to be γ-alumina. The enlarged view of the squared area in (c) is shown in (d), where the calculated plane spacing corresponds to the (222) plane of γ-alumina.

themselves into a rod with a width of 10 nm. The evaluated $d_{XRD}$ of the γ-alumina is 4.0 nm, which agrees well with the crystallites seen in the TEM image. The FFT pattern inserted in (c) was taken from the whole image area. The spots in the FFT pattern form a discontinuous ring, which corresponds to γ-alumina. The enlarged view of the squared area in (c) is shown in (d) where the lattice images of two crystallites can be clearly observed. The calculated plane spacing is 2.28 Å for both crystallites, which corresponds to the (222) plane of γ-alumina.

When the boehmite powder was calcined at 1000 °C for 1 h, δ- and θ-alumina was formed with the morphology shown in Fig. 6. The nanorod morphology remains, and the nanorod grows a little bit wider, *i.e.* to about 15 nm. Crystallites in size of about 5 nm can also be observed on the surface of the nanorods. The evaluated $d_{XRD}$ is 5.9 nm which is in good agreement with the crystallites shown in the image. The morphology of the sample at

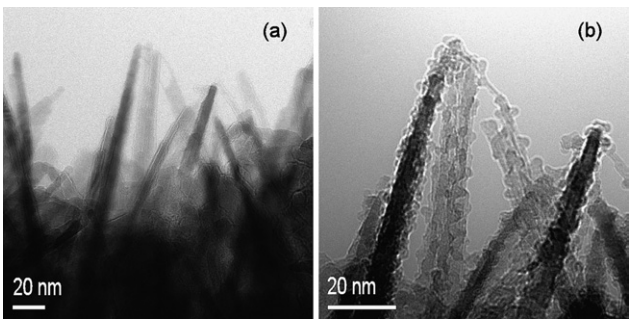


**Fig. 6** TEM images of the alumina prepared by calcining the boehmite starting powder at 1000 °C for 1 h.

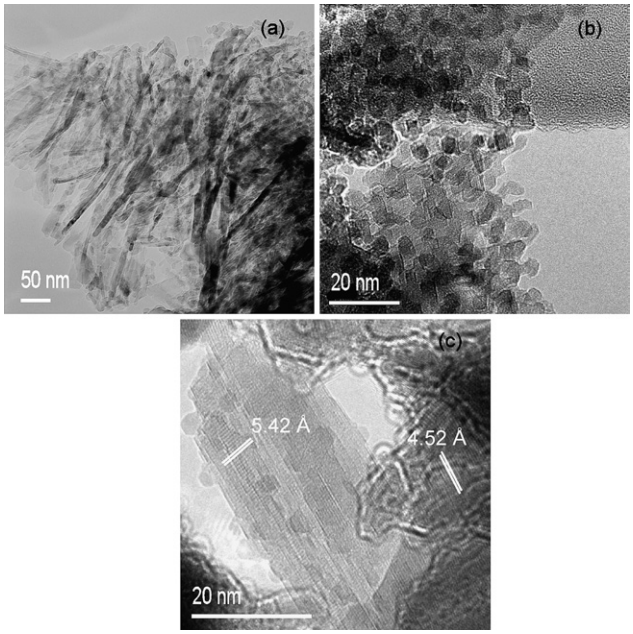


**Fig. 7** TEM images of the alumina prepared by calcining the boehmite starting powder at 1000 °C for 20 h. The plane spacings of 5.42 Å and 4.52 Å correspond to the planes (001) and (201) of θ-alumina.

1000 °C for 1 h follows that of the γ-alumina obtained at 600 °C for 6 h, only with slightly larger crystallites and wider rods.

When the boehmite powder was calcined at 1000 °C for 20 h, α-alumina was formed together with δ- and θ-alumina, with the morphology shown in Fig. 7. The image in a low magnification is shown in (a), where the nanorods grow wider to about 20 nm and some nanoparticles show up. In the image in (b), crystallites at a size of 5 nm can be seen. The evaluated $d_{XRD}$ is 12 nm for δ- and θ-alumina, which is due to the fact that the XRD diffraction peak is not from a single grain. The image (c) shows a nanorod with a width of about 20 nm, where the crystallites at a size of 5 nm can be seen on the surface of the rod. The calculated plane spacings of 5.42 Å and 4.52 Å correspond to the planes (001) and (201) of θ-alumina, respectively.

As reported earlier, when the boehmite starting powder was calcined at 1000 °C for 40 h, pure α-alumina was formed, having morphology of nanorods and nanoparticles. The α-alumina crystallites at a size of 5 nm form into nanorods with varying widths and lengths. By comparing the morphologies of the above tested samples, it seems that morphology remains the same, but phase structure changes, accompanied with grain growth.

### 3.4 Formation scheme of the novel morphology

Based on the XRD, BET and HRTEM studies of the different samples, the hypothetical formation scheme of the nanocrystalline α-alumina with novel morphology is illustrated in Fig. 8. The starting gel powder is of amorphous particles with a high specific surface area of 576 $cm^2/g$. When the gel powder reacts with boiling water, boehmite flakes at a thickness of 5 nm are formed with the crystallites at a size of 3.9 nm. The formation of flakes results from the preferential growth due to the presence of weak hydrogen bonds and interaction between the solvent molecules and the surface $OH^-$ groups *via* hydrogen bonds.[28] When the boehmite powder is calcined at 600 °C for 6 h, the boehmite grains transform into γ-alumina followed by a slight grain growth to 4.0 nm. However, the specific surface area increases from 303 $cm^2/g$ for boehmite to 320 $cm^2/g$ for γ-alumina due to the disintegration of the boehmite flakes and the denser structure of the γ-alumina than boehmite. The γ-alumina crystallites also agglomerate into rods with widths of 10 nm as shown in Fig. 5. The transformation of boehmite into γ-alumina preserves the morphology of boehmite which is a classical example of a topotactic reaction.[29] When the boehmite powder is calcined at 1000 °C for 1 h, the boehmite crystallites transform into δ- and θ-alumina with a slight grain growth to a size of 5.9 nm. The boehmite flakes are disintegrated and more closely agglomerated into wider rods at widths of about 15 nm. The crystallites get aggregated and sintered tightly in the core area of the rods, which is also indicated by the evaluated particle size $d_{BET}$. However, the primary crystallites at a size of 5 nm, still exist in the sample, as shown in Fig. 6. When the boehmite powder is calcined at 1000 °C for 20 h, boehmite crystallites transform into δ-, θ- and α-alumina. With the increase of the dwell time, the primary crystallites of the δ-, θ- and α-alumina grow to bigger secondary crystallites, as indicated by the evaluated $d_{XRD}$. The secondary crystallites then agglomerate and aggregate into large particles and rods as indicated by the evaluated $d_{BET}$. However, the primary crystallites can still be observed in the sample, see Fig. 7. Finally at 1000 °C for 40 h, the boehmite transforms completely into α-alumina where larger rods and particles are formed, however, some primary crystallites in size of about 5 nm can still be observed on the surface of the bigger nanorods and nanoparticles.

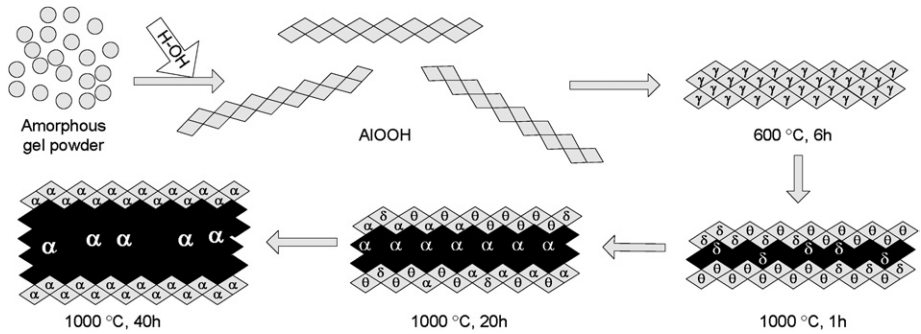


**Fig. 8** Schematic illustration of the formation of the nanocrystalline α-alumina with novel morphology at 1000 °C.

 

To summarize, the boehmite powder obtained *via* a reaction of amorphous gel powder with boiling water plays an important role. Based on the novel synthesis method of the boehmite starting powder, we have a chance to reveal the novel morphology of the obtained nanocrystalline α-alumina.

### 3.5 Phase transformation of θ-alumina to α-alumina

When using boehmite as a starting material to form α-alumina, it passes the series of γ-, δ-, then θ-, and finally α-alumina.[30] The phase transformations between transition aluminas are believed to be topotactic and of relatively low energy.[8,29] However, the phase transformation from θ-alumina to α-alumina involves a change in the oxygen sublattice from cubic to hexagonal close packing and generally happens above ~1200 °C. It is commonly believed that α-alumina is formed by a nucleation and growth mechanism. There are mainly two opinions of the nucleation mechanism from θ-alumina to α-alumina: shear nucleation and diffusional nucleation. The supporters of the shear nucleation mechanism suggest that the θ-alumina crystallites are 'sintered' to a critical size, and then the 'cluster' transforms to α-alumina by shear displacement of the oxygen layers.[31,32] The critical size of θ-alumina ranges from 17 nm to several tens of nm.[32–34] Diffusional nucleation of α-alumina has received little attention as compared to the studies that support shear nucleation; however, one major point supporting the diffusional nucleation is the effect of seeds. Many studies have shown that seeds can lower the formation temperature of α-alumina by providing low energy sites for diffusional nucleation and growth.[35–37] Bagwell[33] studied the role of 'critical size' in the diffusional nucleation and concluded that the 'critical size' is not a prerequisite for α-alumina nucleation, but primarily a result of the incubation time required to produce α-alumina nuclei by diffusional nucleation. Bagwell[33] also suggested that the reported large α-alumina nuclei is not due to the shear of large θ-alumina crystallites, but is due to the difficulties in detecting small nuclei and the rapid growth of the α-alumina after nucleation.

In our study, if there is a 'critical size' of θ-alumina, it will be 5.9 nm which is possibly the smallest 'critical size' observed. However, we saw the trend that with the improvement of the characterization methods, it seems that the 'critical size' is getting smaller and smaller all the time. Therefore of the two existing mechanisms, we find the diffusional nucleation mechanism more consistent with our results and agree with Bagwell that the reported 'critical size' is not a must for α-alumina nucleation, but a result of incubation time needed to form α-alumina nuclei by diffusional nucleation. We propose, based on our results, that α-alumina nucleates at the grain boundaries of the θ-alumina grains and grow into the whole grains, forming the above-called primary crystallites. These primary crystallites then grow together into large secondary crystallites, indicated by $d_{XRD}$. The secondary crystallites then agglomerate and aggregate into even larger particles and rods, indicated by $d_{BET}$. Therefore, when the boehmite powder was calcined at 1000 °C for 40 h, the primary crystallites of α-alumina at a size of 5 nm can be observed together with larger nanorods and nanoparticles which result from the growth of the primary crystallites into secondary crystallites as well as the agglomeration and aggregation of the secondary crystallites. The degree of agglomeration can be possibly lowered by calcinations with a very slow heating rate.[10]

## 4. Conclusions

To conclude, we have reported the detailed synthesis process of the nanocrystalline α-alumina with novel morphology at 1000 °C without any seeding material. The transformation to α-alumina cannot be completed at 900 °C even with a very long dwell time of 160 h. At 1000 °C, a dwell time of 40 h is required to complete the phase transformation to α-alumina, however at 1100 °C only 1 h is required to obtain pure α-alumina. We have also illustrated the formation scheme of the novel morphology of the nanocrystalline α-alumina. The morphology of the starting boehmite powder plays an important role. We have finally discussed the phase transformation mechanism from θ-alumina to α-alumina and found the diffusional nucleation model more consistent with the results in our study. It is supposed that in our study α-alumina nucleates at the grain boundaries of the θ-alumina grains and then grow into the whole grains, forming the so-called primary crystallites. The primary crystallites later grow together into large secondary crystallites, which agglomerate and aggregate into even larger particles and rods. Therefore, when the boehmite starting powder was calcined at 1000 °C for 40 h, α-alumina primary crystallites at a size of 5 nm can be observed together with larger nanorods and nanoparticles which result from the growth of the primary crystallites into secondary crystallites, as well as the agglomeration and aggregation of the secondary crystallites.

## Acknowledgements

The present study was supported by Finnish National Graduate School on New Materials and Processes.

## References

1 J. Li, Y. Wu, Y. Pan, W. Liu, Y. Zhu and J. Guo, *Ceram. Int.*, 2008, **34**, 1539.
2 H. J. Kim, T. G. Kim, J. J. Kim, S. S. Park, S. S. Hong and G. D. Lee, *J. Phys. Chem. Solids*, 2008, **69**, 1521.
3 I. Levin and D. Brandon, *J. Am. Ceram. Soc.*, 1998, **81**, 1995.
4 S. M. Kim, Y. J. Lee, K. W. Jun, J. Y. Park and H. S. Potdar, *Mater. Chem. Phys.*, 2007, **104**, 56.
5 Y. Li, J. Liu and Z. Jia, *Mater. Lett.*, 2006, **60**, 3586.
6 Z. Gan, G. Ning, Y. Lin and Y. Cong, *Mater. Lett.*, 2007, **61**, 3758.
7 M. Thiruchitrambalam, V. R. Palkar and V. Gopinathan, *Mater. Lett.*, 2004, **58**, 3063.
8 S. C. Shen, Q. Chen, P. S. Chow, G. H. Tan, X. T. Zeng, Z. Wang and R. B. H. Tan, *J. Phys. Chem. C*, 2007, **111**, 700.
9 R. M. Laine, J. C. Marchal, H. P. Sun and X. Q. Pan, *Nature Mater*, 2006, **5**, 710.
10 H. Liu, G. Ning, Z. Gan and Y. Lin, *Mater.Lett.*, 2008, **62**, 1685.
11 H. L. Wen and F. S. Yen, *J.Cryst.Growth*, 2000, **208**, 696.
12 J. M. Mchale, A. Auroux, A. J. Perrotta and A. Navrotsky, *Science*, 1997, **277**, 788.
13 J. M. McHale, A. Navrotsky and A. J. Perrotta, *J. Phys. Chem. B*, 1997, **101**, 603.
14 R. S. Zhou and R. L. Snyder, *Acta. Cryst.*, 1991, **B47**, 617.
15 M. Kumagai and G. L. Messing, *J. Am. Ceram. Soc.*, 1984, **67**, c230.
16 J. L. McArdle and G. L. Messing, *J. Am. Ceram. Soc.*, 1993, **76**, 214.
17 H. J. Youn and K. S. Hong, *J. Col. Inter.Sci.*, 1999, **211**, 110.
18 H. K. Farag and F. Endres, *J. Mater. Chem.*, 2008, **18**, 442.
19 X. Zhang, M. Honkanen, E. Levänen and T. Mäntylä, *J. Cryst. Growth*, 2008, **310**, 3674.

20 X. Zhang, M. Honkanen, V. Pore, E. Levänen and T. Mäntylä, *Ceram. Int.*, 2008, DOI: 10.1016/j.ceramint.2008.08.010.
21 X. Zhang, M. Honkanen, M. Järn, J. Peltonen, V. Pore, E. Levänen and T. Mäntylä, *Appl. Surf. Sci.*, 2008, **254**, 5129.
22 X. Zhang, M. Järn, J. Peltonen, V. Pore, T. Vuorinen, E. Levänen and T. Mäntylä, *J. Eur. Ceram. Soc.*, 2008, **28**, 2177.
23 X. Zhang, Y. Ge, S. Hannula, E. Levänen and T. Mäntylä, *J. Mater. Chem.*, 2008, **18**, 2423.
24 K. S. W. Sing, D. H. Everett, R. A. W. Haul, L. Moscou, R. A. Pierotti, J. Rouquerol and T. Siemieniewska, *Pure Appl. Chem.*, 1985, **57**, 603.
25 C. Sangwichien, G. L. Aranovich and M. D. Donohue, *Colloids Surf. A*, 2002, **206**, 313.
26 F. Rouquerol, J. Rouquerol and K. Sing, *Adsorption by Powders and Porous Solids: Principles, Methodology and Applications*, Academic Press, 1999.
27 G. Leofanti, M. Padovan, G. Tozzola and B. Venturelli, *Catal. Today*, 1998, **41**, 207.
28 S. C. Kuiry, E. Megen, S. D. Patil, S. A. Deshpande and S. Seal, *J. Phys. Chem. B*, 2005, **109**, 3868.
29 S. Bhaduri, E. Zhou and S. B. Bhaduri, *Nano Struct. Mater.*, 1996, **7**, 487.
30 L. D. Hart, *Alumina Chemicals: Science and Technology Handbook*, The American Ceramic Society Inc, Westerville, Ohio, 1990, p. 19.
31 G. C. Bye and G. T. Simpkin, *Ibid*, 1974, **76**, 367.
32 J. R. Wynnyckyj and C. G. Morris, *Met. Trans. B*, 1985, **16B**, 345.
33 R. B. Bagwell, G. L. Messing and P. R. Howell, *J. Mater. Sci.*, 2001, **36**, 1833.
34 H. L. Wen and F. S. Yen, *J. Cryst. Growth*, 2000, **208**, 696.
35 M. Kumagai and G. L. Messing, *J. Amer. Ceram. Soc.*, 1985, **68**, 500.
36 J. L. McArdle and G. L. Messing, *Ibid*, 1993, **76**, 214.
37 R. A. Shelleman, G. L. Messing and M. Kumagai, *J. Non-Cryst. Solids*, 1986, **82**, 277.



 